

Unexpectedly Lengthened N–H···Co Hydrogen Bonds?

Lee Brammer,* Juan C. Mareque Rivas, and Dong Zhao

Department of Chemistry, University of Missouri-St. Louis, 8001 Natural Bridge Road, St. Louis, Missouri 63121-4499

Received March 20, 1998

Low-temperature crystal structures of $\text{QuinH}^+\text{Co}(\text{CO})_4^-$, **1** ($\text{QuinH}^+ = \text{quinuclidinium}$), $(\text{DABCO})\text{H}^+\text{Co}(\text{CO})_3\text{P}(\textit{p}\text{-tolyl})_3^-$, **2**, and $(\text{DABCO})\text{H}^+\text{Co}(\text{CO})_3\text{PPh}_2(\textit{p}\text{-tolyl})^-$, **3** ($\text{DABCO} = 1,4\text{-diazabicyclooctane}$), **2** and **3** as their acetonitrile solvates, demonstrate that these salts exhibit intermolecular N–H···Co hydrogen bonding between the cation and anion components. NMR and IR data demonstrate the persistence of these interactions in toluene solution. Such solution-state data, which examine solvated ion pairs, suggest little difference between these salts and the corresponding previously reported salts $(\text{DABCO})\text{H}^+\text{Co}(\text{CO})_3\text{L}^-$ (**4**, $\text{L} = \text{CO}$; **5**, $\text{L} = \text{PPh}_3$). However, in the solid state, the N–H···Co hydrogen bonds in **1–3** are some 0.1–0.15 Å longer than would be predicted from consideration of the structures of **4** and **5** and the aforementioned similarity to **4** and **5** in solution. In previous reports we have shown that major steric or electronic changes to the anion or cation have resulted in substantial changes (0.15–0.3 Å) in the N···Co [H···Co] separation for N–H···Co hydrogen bonds in related $\text{R}_3\text{NH}^+\text{Co}(\text{CO})_3\text{L}^-$ ($\text{L} = \text{CO}, \text{PR}_3$) salts. In this report, we present examples in which small changes are made to the anion or cation remote from the N–H···Co hydrogen bond. In the solid state, the effect of these small changes on this hydrogen bond is subsumed by the effect of changes in the supramolecular structure. This clearly indicates the sensitivity of the geometry of these hydrogen bonds to the overall balance of intermolecular interactions in the solid state and as such is pertinent to current interest in weak (intermolecular) interactions for which characterization by X-ray crystallography is important.

Introduction

Hydrogen bonds are arguably the strongest and most directional of noncovalent interatomic interactions. Such interactions have been studied for decades,¹ yet there are still *many surprises* and there is much yet to understand. The importance of hydrogen bonds has been long established in organic chemistry, including as it pertains to small molecules and macromolecules of biological relevance.^{1a} Applications range from understanding biological structure^{1a} and biochemical mechanisms to the design of new materials based upon hydrogen-bonded networks.²

Over the past decade, emerging research has brought to light the importance of hydrogen bonds in inorganic chemistry and particularly in transition metal chemistry.³ The emphasis has

been twofold, stressing hydrogen bonds involving metal-bound ligands,⁴ which in some cases may exhibit characteristics not prevalent in organic chemistry,⁵ and, more pertinent to the present work, introducing the idea that transition metals can themselves participate directly in hydrogen bonding.^{6–8} In recent years, we and others have reported a number of transition metal complexes in which electron-rich, low-oxidation-state late

* E-mail: lee.brammer@umsl.edu.

- (1) Jeffrey, G. A.; Saenger, W. *Hydrogen Bonding in Biological Structures*; Springer-Verlag: Berlin, 1991. (b) Jeffrey, G. A. *An Introduction to Hydrogen Bonding*; Oxford University Press: Oxford, 1997.
- (a) Desiraju, G. R. *Crystal Engineering: The Design of Organic Solids*; Elsevier: Amsterdam, 1989. (b) Sharma, C. V. K.; Desiraju, G. R. In *Perspectives in Supramolecular Chemistry. The Crystal as a Supramolecular Entity*; Desiraju, G. R., Ed.; Wiley: New York, 1996. (c) Aakeröy, C. B. *Acta Crystallogr.* **1997**, *B53*, 569. (d) Subramanian, S.; Zawarotko, M. J. *Coord. Chem. Rev.* **1994**, *137*, 357.
- For pertinent reviews see: (a) Brammer, L.; Zhao, D.; Ladipo, F. T.; Braddock-Wilking, J. *Acta Crystallogr.* **1995**, *B51*, 632. (b) Mareque Rivas, J. C.; Brammer, L. *Coord. Chem. Rev.*, in press. (c) Shubina, Ye. S.; Epstein, L. M. *J. Mol. Struct.* **1992**, *265*, 367. (d) Epstein, L. M.; Shubina, E. S. *Metallorg. Khim.* **1992**, *5*, 61 (English translation, *Organomet. Chem. USSR*, **1992**, *5*, 1). (e) Canty, A. J.; van Koten, G. *Acc. Chem. Res.* **1995**, *28*, 406. (f) Crabtree, R. H.; Siegbahn, P. E. M.; Eisenstein, O.; Rheingold, A. L.; Koetzle, T. F. *Acc. Chem. Res.* **1996**, *29*, 348. (g) Braga, D.; Grepioni, F. *Acc. Chem. Res.* **1997**, *30*, 81. (h) Burrows, A. D.; Chan, C.-W.; Chowdry, M. M.; McGrady, J. E.; Mingos, D. M. P. *Chem. Soc. Rev.* **1995**, *24*, 329. (i) Raymo, F. M.; Stoddart, J. F. *Chem. Ber.* **1996**, *129*, 981.

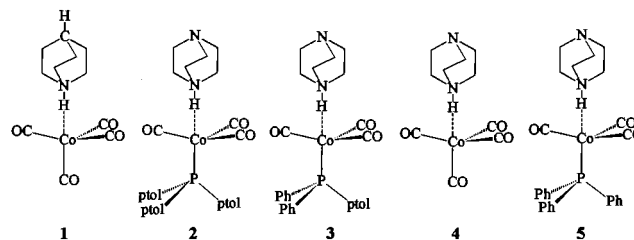
- (4) (a) Braga, D.; Grepioni, F.; Sabatino, P.; Desiraju, G. R. *Organometallics* **1994**, *13*, 3532. (b) Braga, D.; Biradha, K.; Grepioni, F.; Pedireddi, V. R.; Desiraju, G. R. *J. Am. Chem. Soc.* **1995**, *117*, 3156. (c) Biradha, K.; Desiraju, G. R.; Braga, D.; Grepioni, F. *Organometallics* **1996**, *15*, 1284.
- (5) Auallón, G.; Bellamy, D.; Brammer, L.; Bruton, E. A.; Orpen, A. G. *Chem. Commun.* **1998**, 653.
- (6) (a) Brammer, L.; Charnock, J. M.; Goggin, P. L.; Goodfellow, R. J.; Orpen, A. G.; Koetzle, T. F. *J. Chem. Soc., Dalton Trans.* **1991**, 1789. (b) Brammer, L.; McCann, M. C.; Bullock, R. M.; McMullan, R. K.; Sherwood, P. *Organometallics* **1992**, *11*, 2339. (c) Brammer, L.; Zhao, D. *Organometallics* **1994**, *13*, 1545. (d) Zhao, D.; Ladipo, F. T.; Braddock-Wilking, J.; Brammer, L.; Sherwood, P. *Organometallics* **1996**, *15*, 1441.
- (7) (a) Calderazzo, F.; Fachinetti, G.; Marchetti, F.; Zanazzi, P. F. *J. Chem. Soc., Chem. Commun.* **1981**, 181. (b) Wehman-Ooyevaar, I. C. M.; Grove, D. M.; Kooijman, H.; van der Sluis, P.; Spek, A. L.; van Koten, G. *J. Am. Chem. Soc.* **1992**, *114*, 9916. (c) Wehman-Ooyevaar, I. C. M.; Grove, D. M.; de Vaal, P.; Dedieu, A.; van Koten, G. *Inorg. Chem.* **1992**, *31*, 5484. (d) Kazarian, S. G.; Hamley, P. A.; Poliakov, M. J. *J. Am. Chem. Soc.* **1993**, *115*, 9069. (e) Albinati, A.; Lianza, F.; Pregosin, P. S.; Müller, B. *Inorg. Chem.* **1994**, *33*, 2522. (f) Albinati, A.; Lianza, F.; Müller, B.; Pregosin, P. S. *Inorg. Chim. Acta* **1993**, *208*, 119. (g) Shubina, E. S.; Krylov, A. N.; Timofeeva, T. V.; Struchkov, Yu. T.; Ginzburg, A. G.; Loim, N. M.; Epstein, L. M. *J. Organomet. Chem.* **1992**, *434*, 329. (h) Shubina, E. S.; Krylov, A. N.; Kreindlin, A. Z.; Rybinskaya, M. I.; Epstein, L. M. *J. Organomet. Chem.* **1994**, *465*, 259. (i) Epstein, L. M.; Krylov, A. N.; Shubina, E. S. *J. Mol. Struct.* **1994**, *322*, 345. (j) Braga, D.; Grepioni, F.; Tedesco, E.; Biradha, K.; Desiraju, G. R. *Organometallics* **1997**, *16*, 1846. (k) Gao, Y.; Eisenstein, O.; Crabtree, R. H. *Inorg. Chim. Acta* **1997**, *254*, 105.

transition metals serve as hydrogen bond *acceptors*,^{6,7} participating directly in the three-center hydrogen bonding interaction, D–H···ML_n (D = hydrogen bond donor). Conversely, in some circumstances, transition metal hydrides have been shown to act as hydrogen bond *donors*,⁸ L_nM–H···A (A = hydrogen bond acceptor). Such systems are clearly relevant to an understanding of protonation/deprotonation of metal centers and have been implicated in such reactions.^{7b,h,i} We have also previously suggested that D–H···ML_n hydrogen bonds may play a role in (stepwise, heterolytic) oxidative addition reactions at some metal centers.^{3a} In related systems, the propensity of hydridic metal hydrides to form hydrogen bonds of the type D–H···H–ML_n has been clearly demonstrated by Crabtree and co-workers^{3f,9} and by other groups,¹⁰ and the role of such hydrogen bonds in the protonation of metal hydrides and deprotonation of metal dihydrogen complexes is implicated.^{9b}

Our previous studies of salts of the type R₃NH⁺Co(CO)₃L[−] (L = CO, PPh₃)^{6b–d} have focused on such salts in which the cation and anion are linked via an N–H···Co hydrogen bond. The length of this hydrogen bond has been shown to be substantially affected by the steric demands of the amine donor and the basicity of the cobalt center (H bond acceptor). Thus, on changing from a somewhat sterically demanding amine, Et₃N, to one that is less so, e.g., Me₃N or DABCO (DABCO = 1,4-diaza[2.2.0]bicyclooctane), the N···Co [H···Co] separation is reduced by ca. 0.3 Å.^{6b,d,7a} This separation is further reduced by ca. 0.15 Å for the Co(CO)₃L[−] anion when changing from L = CO to L = PPh₃.^{6d} In both cases this determination was made by X-ray crystallography. In the latter case, spectroscopic measurements in solution and theoretical calculations confirmed that the change in length was also associated with a change in strength of the hydrogen bond of the isolated ion pair.^{6d}

The present work describes the spectroscopic and crystallographic characterization of three compounds, (Quin)H⁺Co(CO)₄[−], **1** (Quin = quinuclidine), (DABCO)H⁺Co(CO)₃P(*p*-tolyl)₃[−], **2**, and (DABCO)H⁺Co(CO)₃PPh₂(*p*-tolyl)[−], **3** (Chart 1). These compounds differ electronically in only a minor way from either (DABCO)H⁺Co(CO)₄[−] **4** or (DABCO)H⁺Co(CO)₃PPh₃[−] **5**, which we have reported previously,^{6d} and are sterically equivalent to **4** and **5** in the vicinity of the donor (N–H) and acceptor (Co). In contrast to the minor differences indicated by solution spectroscopy in the geometry of the ion pairs of **1** relative to **4** and of **2** or **3** relative to **5**, substantial differences in the solid-state geometry of the N–H···Co hydrogen bond are observed. Indeed, perturbation of the N–H···Co geometry

Chart 1. N–H···Co Hydrogen-Bonded “Molecular” Structures of **1–5** (ptol = *p*-tolyl).



in the present systems (relative to **4** or **5**) is of similar magnitude as that observed as a result of major steric and/or electronic changes noted earlier (*vide supra*).

In work of some relevance to the present study, Orpen and Martín have shown recently that even *intramolecular* geometries in the solid-state, i.e., covalent bond lengths, angles, etc., can be affected substantially by their molecular and crystal environment.¹¹ Maseras, Eisenstein, Caulton, and co-workers have also recently demonstrated the unexpected effect of substituent steric bulk in *promoting* the formation of agostic interactions for which electronic factors alone were insufficient to explain.¹² The present work provides another example of the perturbing effect of interactions *remote* from that which is the focus of attention. The consequences of this finding are discussed in the broader context of current interest in weak interactions in inorganic chemistry.

Experimental Section

General Procedures and Instrumentation. All manipulations of oxygen- and/or water-sensitive materials were carried out under an atmosphere of argon either using Schlenk-line techniques or in a Vacuum Atmospheres drybox. NMR spectra were recorded on a Bruker ARX-500 spectrometer. IR spectra were recorded on either a Perkin-Elmer 1600 series or Mattson 6020 FT-IR spectrometer.

(Quinuclidine)H⁺Co(CO)₄[−] **1.** (Quinuclidine)H⁺Co(CO)₄[−] was prepared in a manner similar to that used for related R₃NH⁺Co(CO)₄[−] species.⁶ In a typical reaction, Co₂(CO)₈ (0.75 g, 2.19 mmol) was dissolved in hexane (20 mL) and, at room temperature, *N,N*-dimethylformamide (5 mL, 64 mmol) was added. The solution was stirred for 1 h, after which two layers had formed; the upper layer was colorless and the bottom one pink. The solution was cooled to −78 °C, and 5 mL of 1 M HCl solution was slowly added. After the addition was completed, the solution was allowed to warm and was stirred for 15 min, yielding a pale yellow top layer (HCo(CO)₄) and a blue bottom layer (CoCl₂). The blue layer was removed, and the yellow solution was washed three times with equal portions of degassed H₂O (10 mL) and afterward dried at −78 °C over P₂O₅ for 30 min. The dry yellow solution containing the HCo(CO)₄ was added to a toluene solution (30 mL) of quinuclidine (0.24 g, 2.15 mmol) at liquid nitrogen temperature. Once the addition was completed, the solution was allowed to slowly warm back to room temperature, resulting in the immediate formation of a white precipitate, which was separated and dried under reduced pressure. Crystals were grown from a toluene solution of the white powder, which was also used for the spectroscopic characterization. ¹H NMR: (500 MHz, C₆D₅CD₃, 298 K) δ 2.34 (m, CH₂), 0.90 (septet, CH), 0.71 (m, CH₂), 9.8 (br, N–H); (500 MHz, C₆D₅CD₃, 188 K) δ 2.15 (m, CH₂), 0.84 (septet, CH), 0.61 (m, CH₂), 9.4 (br, N–H). ¹³C NMR: (125.7 MHz, C₆D₅CD₃, 298 K) δ 46.1 (s, N–CH₂), 22.3 (s, C–CH₂), 19.0 (s, CH), no signal observed for CO ligands; (125.7 MHz, C₆D₅CD₃, 193 K) δ 45.4 (s, N–CH₂), 21.7 (s, C–CH₂), 18.2 (s, CH),

- (8) (a) Adams, M. A.; Folting, K.; Huffman, J. C.; Caulton, K. G. *Inorg. Chem.* **1979**, *18*, 3020. (b) Epstein, L. M.; Shubina, E. S.; Krylov, A. N.; Kreindlin, A. Z.; Rybinskaya, M. I. *J. Organomet. Chem.* **1993**, *447*, 277. (c) Fairhurst, S. A.; Henderson, R. A.; Hughes, D. L.; Ibrahim, S. K.; Pickett, C. J. *J. Chem. Soc., Chem. Commun.* **1995**, 1569. (d) Peris, E.; Crabtree, R. H. *J. Chem. Soc., Chem. Commun.* **1995**, 2179. (e) Braga, D.; Grepioni, F.; Tedesco, E.; Biradha, K.; Desiraju, G. R. *Organometallics* **1996**, *15*, 269.
- (9) (a) Lee, J. C.; Peris, E.; Rheingold, A. L.; Crabtree, R. H. *J. Am. Chem. Soc.* **1994**, *116*, 11014. (b) Peris, E.; Lee, J. C.; Rambo, J. R.; Eisenstein, O.; Crabtree, R. H. *J. Am. Chem. Soc.* **1995**, *117*, 3485. (c) Peris, E.; Wessel, J.; Patel, B. P.; Crabtree, R. H. *J. Chem. Soc., Chem. Commun.* **1995**, 2175. (d) Wessel, J.; Lee, J. C., Jr.; Peris, E.; Yap, G. P. A.; Fortin, J. B.; Ricci, J. S.; Sini, G.; Albinati, A.; Koetzle, T. F.; Eisenstein, O.; Rheingold, A. L.; Crabtree, R. H. *Angew. Chem., Int. Ed. Engl.* **1995**, *34*, 2507. (e) Richardson, T. B.; Koetzle, T. F.; Crabtree, R. H. *Inorg. Chim. Acta* **1996**, *250*, 69.
- (10) (a) Stevens, R. C.; Bau, R.; Milstein, D.; Blum, O.; Koetzle, T. F. *J. Chem. Soc., Dalton Trans.* **1990**, 1429. (b) Park, S.; Ramachandran, R.; Lough, A. J.; Morris, R. J. *Chem. Soc., Chem. Commun.* **1994**, 2201. (c) Lough, A. J.; Park, S.; Ramachandran, R.; Morris, R. J. *Am. Chem. Soc.* **1994**, *116*, 8356. (d) Shubina, E. S.; Belkova, N. V.; Krylov, A. N.; Vorontsov, E. V.; Epstein, L. M.; Gusev, D. G.; Niedermann, M.; Berke, H. *J. Am. Chem. Soc.* **1996**, *118*, 1105.

- (11) (a) Martín, A.; Orpen, A. G. *J. Am. Chem. Soc.* **1996**, *118*, 1464. (b) Martín, A.; Orpen, A. G. *Trans. Am. Crystallogr. Assoc.* **1995**, *31*, 31.
- (12) Ujaque, G.; Cooper, A. C.; Maseras, F.; Eisenstein, O.; Caulton, K. G. *J. Am. Chem. Soc.* **1998**, *120*, 361.

Table 1. Data Collection, Structure Solution, and Refinement Parameters for 1–3

	1	2	3
cryst color, habit	colorless, prisms	yellow, triangular prism	yellow, prisms
cryst size (mm)	0.17 × 0.17 × 0.05	0.22 × 0.18 × 0.10	0.45 × 0.40 × 0.20
cryst syst	triclinic	triclinic	monoclinic
space group, Z	$P\bar{1}$, 2	$P\bar{1}$, 2	$P2_1/c$, 4
a (Å)	7.1156(1)	9.4915(1)	9.144(5)
b (Å)	9.4351(1)	10.8733(2)	18.229(9)
c (Å)	9.5947(1)	15.7902(2)	17.280(9)
α (deg)	80.511(1)	95.065(1)	90
β (deg)	81.006(1)	106.349(1)	92.34(4)
γ (deg)	86.079(1)	99.474(1)	90
V (Å ³)	626.93(2)	1526.71(4)	2878(3)
density (g/cm ³)	1.500	1.308	1.324
temp (K)	208(5)	143(5)	143(5)
μ(Mo Kα) (mm ⁻¹)	1.370	0.650	0.687
θ range (deg)	2.18–29.81	1.36–32.48	1.62–24.99
reflns collected	9464	35797	5408
indep reflns, n (R _{int})	3273 (0.030)	10097 (0.065)	5067 (0.147)
obsd (I > 2.0σ(I))	2855	6508	1752
least-squares params (p)	210	374	330
restraints (r)	0	0	139
R1(F), ^a wR2(F ²) ^a (I > 2.0σ(I))	0.031, 0.076	0.054, 0.108	0.116, 0.215
S(F ²) ^a (I > 2.0σ(I))	1.055	1.29	1.28

$$^a R1(F) = \sum(|F_o| - |F_c|) / \sum|F_o|; wR2(F^2) = [\sum w(F_o^2 - F_c^2)^2 / \sum w F_o^4]^{1/2}; S(F^2) = [\sum w(F_o^2 - F_c^2)^2 / (n - p)]^{1/2}.$$

no signal observed for CO ligands. IR (cm⁻¹): (CD₃CN) ν(CO) 1891 (s); (C₆D₅CD₃) ν(CO) 2020 (w), 1931 (w), 1896 (s).

(DABCO)H⁺Co(CO)₃P(*p*-tolyl)₃⁻ 2. (DABCO)H⁺Co(CO)₃P(*p*-tolyl)₃⁻ was prepared as noted previously for (DABCO)H⁺Co(CO)₃PPh₃⁻.^{6d} Thus, HCo(CO)₄ prepared in situ, as described for **1**, was first vacuum transferred to a toluene solution containing 1 equiv of the phosphine ligand and stirred for 1 h prior to the introduction of 1 equiv of the diamine. Compound **2** was isolated as its acetonitrile solvate, a yellow crystalline product, by direct crystallization at -23 °C from an acetonitrile solution of the crude mixture of products that included the phosphine-substituted cobalt carbonyl hydride HCo(CO)₂(P(*p*-tolyl)₃)₂ (identified in the ¹H NMR of the crude product by a signal at ca. δ -10, with coupling to the ³¹P nuclei) and some decomposition products. Crystals were selected for use in the X-ray diffraction study, and the remaining crystals of **2** were redissolved for spectroscopic characterization. ¹H NMR: (500 MHz, C₆D₅CD₃, 298 K) δ 2.36 (s, CH₂); (500 MHz, C₆D₅CD₃, 188 K) δ 2.31 and 1.73 (s, CH₂), 13.2 (s, NH); (500 MHz, CD₃CN, 298 K) δ 2.94 (s, CH₂); (500 MHz, CD₃CN, 240 K) δ 2.91 (s, CH₂). ¹³C NMR: (125.7 MHz, C₆D₅CD₃, 298 K) δ 46.8 (s, CH₂), no signal observed for CO ligands; (125.7 MHz, C₆D₅-CD₃, 193 K) δ 43.5 (s, CH₂), no signal observed for CO ligands. ³¹P NMR: (202.5 MHz, C₆D₅CD₃, 298 K) δ 57.7; (202.5 MHz, C₆D₅CD₃, 188 K) δ 60.0. IR (cm⁻¹): (CD₃CN) ν(CO) 1925 (w), 1834 (s); (C₆D₅-CD₃) ν(CO) 1965 (w), 1856 (m).

(DABCO)H⁺Co(CO)₃PPh₂(*p*-tolyl)⁻ 3. (DABCO)H⁺Co(CO)₃PPh₂(*p*-tolyl)⁻ was prepared in the same manner as **2** and again isolated as its acetonitrile solvate, a yellow crystalline product, by direct crystallization at -23 °C from an acetonitrile solution of the crude mixture of products. Crystals were selected for the X-ray diffraction study, and the remaining crystals of **3** were redissolved for spectroscopic characterization. ¹H NMR: (500 MHz, C₆D₅CD₃, 298 K) δ 2.29 (s, CH₂); (500 MHz, C₆D₅CD₃, 188 K) δ 2.31 and 1.73 (s, CH₂), 13.1 (s, NH). ¹³C NMR: (125.7 MHz, C₆D₅CD₃, 298 K) δ 46.4 (s, CH₂), no signal observed for CO ligands; (125.7 MHz, C₆D₅CD₃, 193 K) δ 43.7 (v br s, CH₂), no signal observed for CO ligands. ³¹P NMR: (202.5 MHz, C₆D₅CD₃, 298 K) δ 60.1; (202.5 MHz, C₆D₅CD₃, 188 K) δ 61.6. IR (cm⁻¹): (CD₃CN) ν(CO) 1926 (w), 1834 (s); (C₆D₅CD₃) ν(CO) 1968 (w), 1849 (m).

X-ray Crystal Structure Determinations of 1–3. Intensity data for **1** and **3** were collected using a Siemens SMART CCD-based area detector diffractometer. Data for **2** were obtained using a Siemens R3m/V diffractometer. In each case, graphite-monochromated Mo Kα radiation was used. The compounds decompose rapidly in air even in the solid state. Thus, crystals were first coated in hydrocarbon oil in the drybox and subsequently mounted on glass fibers and rapidly

Table 2. Selected Interatomic Distances (Å) and Angles (deg) for 1–3

	1	2	3
Co–P		2.198(1)	2.177(3)
Co–C(1)	1.772(2)	1.742(2)	1.71(2)
Co–C(2)	1.757(2)	1.743(3)	1.74(2)
Co–C(3)	1.771(2)	1.739(2)	1.705(14)
Co–C(4) ^a	1.777(2)		
Co···N	3.563(2)	3.372(2)	3.347(6)
C(1)–O(1)	1.151(2)	1.170(3)	1.18(2)
C(2)–O(2)	1.153(2)	1.157(3)	1.16(2)
C(3)–O(3)	1.152(2)	1.171(3)	1.175(14)
C(4)–O(4) ^a	1.150(2)		
P–C(11)		1.849(2)	1.828(12)
P–C(21)		1.832(2)	1.836(12)
P–C(31)		1.839(2)	1.829(12)
P–Co–C(1)		108.00(8)	99.9(5)
P–Co–C(2)		102.86(8)	107.9(5)
P–Co–C(3)		103.46(7)	101.9(4)
C(1)–Co–C(2)	110.60(8)	113.69(12)	118.1(7)
C(1)–Co–C(3)	113.55(8)	112.45(11)	112.0(7)
C(1)–Co–C(4)	107.74(8)		
C(2)–Co–C(3)	110.93(7)	115.10(12)	114.4(8)
C(2)–Co–C(4)	107.49(8)		
C(3)–Co–C(4)	107.74(8)		

^a Axial CO.

transferred to the cold nitrogen stream of the diffractometer. For each compound, intensity data sets were collected for at least two different crystals. The refinements based upon the best of these data sets are presented herein.

Data for **1** and **3** were corrected for absorption using empirical methods based upon the method of Blessing;¹³ data for **2** were corrected by semiempirical methods.¹⁴ Each crystal structure was solved by direct methods and refined to convergence against *F*² data (*F*² > -3σ(*F*²)) using the SHELXTL suite of programs.¹⁴ For **1**, all non-hydrogen atoms were refined anisotropically. All hydrogen atoms were located directly from the difference map and refined using unconstrained positional parameters and fixed isotropic displacement parameters. For **2**, all non-hydrogen atoms were refined anisotropically, ammonium hydrogen, H(1), was refined isotropically, and all methylene hydrogens were refined using a riding model with fixed isotropic displacement

(13) Blessing, R. H. *Acta Crystallogr.* **1995**, *A51*, 33.

(14) *SHELXTL 5.0*; Siemens Analytical X-ray Instruments, Inc.: Madison, WI, 1995.

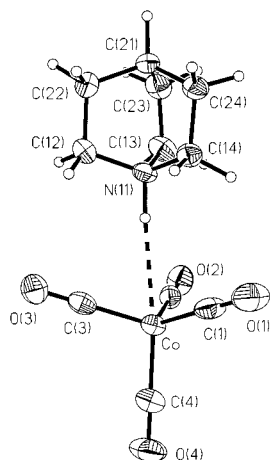


Figure 1. Molecular structure of **1** shown with 50% probability ellipsoids for non-hydrogen atoms.

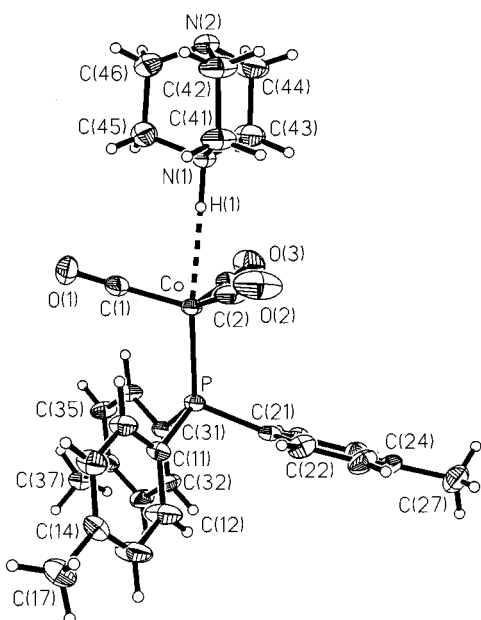


Figure 2. Molecular structure of **2** shown with 50% probability ellipsoids for non-hydrogen atoms.

parameters. For **3**, the DABCO moiety exhibits orientational disorder about the N...N axis (staggered with respect to the carbonyl groups, 72%; eclipsed with respect to the carbonyl groups, 28%). The PPh₂-(*p*-tolyl) ligand is also orientationally disordered such that the methyl group is associated with two of the aromatic rings in a 71:29 ratio. Non-hydrogen atoms were refined anisotropically using appropriate constraints and restraints. The positional parameters of ammonium hydrogen, H(1), were refined freely (U_{iso} fixed); all other hydrogens were refined using a riding model with fixed isotropic displacement parameters.

Experimental data pertinent to the structure determinations are given in Table 1, selected interatomic distances and angles are presented in Table 2, and the molecular structures are presented in Figures 1–3.

Results

Compounds **1**–**3** have been characterized in the solid state by low-temperature X-ray crystallography and further characterized in solution by variable temperature NMR spectroscopy and by IR spectroscopy. The solution-state characterization is of solvated N—H...Co hydrogen-bonded ion pairs or solvent-separated ions, depending upon the polarity of the solvent. However, the crystallographic characterization describes the same N—H...Co hydrogen-bonded ion pairs subjected to

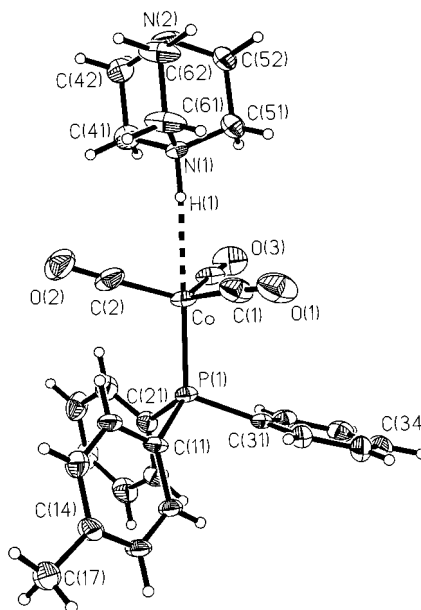


Figure 3. Molecular structure of **3** showing major components of disordered regions. Non-hydrogen atoms are represented by 30% probability ellipsoids.

interactions involving nearest-neighbor cations and anions. The focus of this report is the difference of the observed N—H...Co geometries of **1**–**3** in the solid state from those anticipated based upon (i) structural characterization of similar salts **4** and **5** and (ii) a comparison of solution-state spectroscopic characterization of the hydrogen-bonded ion pairs with those of **4** and **5**.

Spectroscopic Studies in Solution. The carbonyl region of the IR spectra for **1** shows no significant difference from that of the related **4**.^{6d} In **1**, the absence of the N—H...Co hydrogen bond is indicated by a single (T_2) carbonyl band consistent with an isolated anion of T_d symmetry. The presence of the hydrogen bond in nonpolar solvents results in distortion of the anion geometry to C_{3v} symmetry and gives rise to three observable carbonyl bands ($2A_1 + E$). The carbonyl regions of the IR spectra for **2** and **3** show the C_{3v} symmetry of the anion in both polar (CD_3CN) and nonpolar ($C_6D_5CD_3$) solvents ($2A_1 + E$ bands) and exhibit $\nu(CO)$ stretching vibrations at approximately the same wavenumbers as previously noted for **5**.^{6d} This indicates no perceptible difference in back-donation to the CO ligands, thus suggesting no observable difference, by this technique, in basicity at the metal center due to exchanging phenyl for *p*-tolyl groups in the phosphine ligands. As in previously reported related species, a $\nu(N-H)$ band could not be unambiguously identified for **1**–**3**.

The ¹H NMR spectrum for **1** (as an N—H...Co hydrogen-bonded ion pair) in toluene-*d*₈ solution shows signals for the three types of CH protons. Analogous to the earlier study of **4**, these protons are shifted upfield upon a reduction in the temperature and lie *upfield* of the signals for free quinuclidine. For **1**, it is clear that the protons closest to the N—H...Co hydrogen bond undergo the largest shift (¹H NMR δ at 298 K is 2.34, 0.90, and 0.71, while at 188 K, it is 2.15, 0.84, and 0.61, presented in order of decreasing proximity to the nitrogen). The downfield N-H signal is typical of this class of salts and is most sensitive to changes in temperature and/or concentration.

¹H NMR studies of **2** and **3** in toluene-*d*₈ solution indicate behavior related to that of **1** but most similar to that of **5**.^{6d} At room temperature, only a singlet is observed for the methylene protons of the cation at ca. 2.3 ppm, indicative of a fluxional

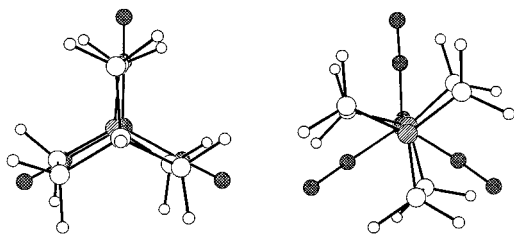


Figure 4. Views of **1** and **4** illustrating eclipsed and staggered conformations, respectively. $\text{Co}(\text{CO})_4^-$ anions are shaded with cross-hatching; nitrogens of the cation are shaded with diagonal lines.

process discussed previously^{6d} in which the $\text{N}-\text{H}\cdots\text{Co}$ hydrogen bond is broken. The chemical shift is also indicative of the close proximity of the anion, which causes the signal to shift to slightly *upfield* of the corresponding resonance for free DABCO (2.4 ppm).^{3a} Upon a decrease in the temperature, the methylene signal shifts further upfield and broadens then splits into separate signals corresponding to the sets of methylene groups at the two ends of the cation, as is observed for **5**. However, at coalescence, the broadened signal overlaps with the methyl signal of the protio-solvent impurity, rendering precise measurement of the coalescence temperature unfeasible. Nevertheless, it is clear that the coalescence point lies in the temperature range 213–253 K and thus must be similar to that observed for $(\text{DABCO})\text{H}^+\text{Co}(\text{CO})_3\text{PPh}_3^-$ (ca. 235 K). Thus, consistent with the conclusion from the IR data, one must conclude that the replacement of phenyl substituents by *p*-tolyl groups has at best only a small effect upon the strength of the $\text{N}-\text{H}\cdots\text{Co}$ hydrogen bond in the isolated solution ion pair and thus presumably on the basicity of the cobalt center. In this regard, it should be noted that the importance of electronic aspects of Lewis acid–base interactions can sometimes be overemphasized, as seen in a recent study of agostic interactions at very electron deficient metal centers where steric effects were determined to be at least as important.¹²

Finally, it should also be noted that ^1H NMR spectra of **2** and **3** in CD_3CN solution, where the salts exist as solvent-separated ions, show no upfield shift or broadening of the methylene signal upon a decrease in the temperature. Furthermore, in the absence of the close interaction with the anion, these protons resonate at ca. 2.9 ppm over the temperature range 300–240 K. This is *downfield* of the signal for free DABCO and more typical of CH protons adjacent to an ammonium center.

Crystal Structure of 1. The structure of the hydrogen-bonded ion pair for **1** shows marked differences from that of the $(\text{DABCO})\text{H}^+\text{Co}(\text{CO})_4^-$ analogue **4** reported earlier.^{6d} Although the two amines, quinuclidine and DABCO, are very similar sterically and quite similar electronically (*viz.* amine basicity), the structural features of the two salts are on the contrary rather different. In both cases, the cation and anion are linked via an approximately linear $\text{N}-\text{H}\cdots\text{Co}$ hydrogen bond (172.4° in **1**¹⁵). However, the $\text{N}\cdots\text{Co}$ [$\text{H}\cdots\text{Co}$]¹⁵ separation in **1** is some 0.13 Å longer than that in **4** (3.563(2) [2.519] vs 3.437(3) [2.392] Å). Furthermore, while in **4** the three “equatorial” carbonyls are staggered about the $\text{N}\cdots\text{Co}$ vector with respect to the methylene groups attached to the ammonium nitrogen, in **1**, the conformation is eclipsed (Figure 4). It is reasonable to presume that the lowest energy arrangement for a single isolated ion pair should be similar to that observed in

the crystal structure of **4**. Thus, since a crystal represents an energetic balance of intermolecular interactions, formation of the higher energy (elongated and eclipsed) form of the ion pair observed in **1** must be compensated by other interactions in the solid state. The crystal structures of both **1** and **4** exhibit extensive networks of cation–anion $\text{C}-\text{H}\cdots\text{O}$ hydrogen bonds, and recent attention has been drawn to the importance of such interactions in determining the arrangement of organometallic molecules and ions in the solid state.^{3g,4b} However, we cannot expect to be able to point to a specific intermolecular interaction that provides the energetic compensation inferred for the structure of **1**. Nevertheless, the differences between **1** and **4** that most probably contribute to this effect can be highlighted. Thus, the single chemical difference between **1** and **4** is the replacement of a potential hydrogen bond acceptor (N) in **4** by a potential hydrogen bond donor (C–H) in **1**. This necessitates a change in the packing arrangement of the cations and anions; as in the crystal structures of **1** and **4**, these sites are active in hydrogen bond formation.

Crystal Structures of 2 and 3. Although crystallized as their acetonitrile solvates, **2** and **3** exhibit molecular structures “similar” to that of the related species $(\text{DABCO})\text{H}^+\text{Co}(\text{CO})_3\text{PPh}_3-$ **5**.^{6d} Thus, an approximately linear intermolecular $\text{N}-\text{H}\cdots\text{Co}$ hydrogen bond [177.4°, **2**; 175.5°, **3**]¹⁵ lies *trans* to the phosphine ligand (Figures 2 and 3), and the angles between the phosphine and carbonyl ligands are substantially decreased from 109.5° in order to accommodate the hydrogen bond. Surprisingly, the previously observed trend of shorter hydrogen bonds upon increasing the basicity of the metal center^{6d} is not continued in **2** and **3**, which exhibit $\text{N}\cdots\text{Co}$ [and $\text{H}\cdots\text{Co}$]¹⁵ separations, 3.371(2) [2.32 Å] for **2** and 3.347(6) [2.30 Å] for **3**, slightly greater than those of the triphenylphosphine-substituted analogue **5**, 3.294(6) [2.25 Å], though still appreciably shorter than those of parent tetracarbonylcobaltate species **4** (*vide supra*). As in **5**, the bond angles of the anions in **2** and **3** also deviate by up to a few degrees from those of the idealized C_3 symmetry. Again, one has to look to the ensemble of intermolecular interactions in these structures to provide an explanation for the unexpectedly lengthened $\text{N}-\text{H}\cdots\text{Co}$ hydrogen bonds in **2** and **3**. As already noted for **1** and **4**, the crystal structures of **2** and **3** (and **5**) possess extensive networks of $\text{C}-\text{H}\cdots\text{O}$ hydrogen bonds, and it is inevitably the energetic balance of these and other (van der Waals) interactions that permits the observed variability of the $\text{N}-\text{H}\cdots\text{Co}$ hydrogen bond length across this series of structures. The most obvious differences between the crystal structures of **2** and **3** and that of **5** are replacement of phenyl groups by *p*-tolyl groups at the molecular level and the incorporation of acetonitrile solvent molecules in the structures of **2** and **3** at the supramolecular level. However, as in the case of **1** and **4**, one can only identify these differences and cannot expect to identify a specific interaction or interactions that account for the difference in $\text{N}-\text{H}\cdots\text{Co}$ hydrogen bond geometries across this series.

Discussion

X-ray crystallography remains a major tool for studying hydrogen-bonding interactions despite the well-known limitations of this technique in precisely locating hydrogen atoms. Indeed, the relative strengths of individual hydrogen bonds are sometimes inferred from their geometry in a crystalline solid material. However, this is a practice fraught with problems. Hydrogen bonds, although stronger than most intermolecular interactions, are clearly weak bonds (typically <10 kcal/mol). Thus, their geometry can be anticipated to be quite sensitive to

(15) Calculated by extending (or contracting) the $\text{N}-\text{H}$ distance along the determined $\text{N}-\text{H}$ vector to yield a value of 1.05 Å as determined by neutron diffraction for $\text{Et}_3\text{NH}^+\text{Co}(\text{CO})_4^-$.^{6b}

the surroundings, where among other factors the existence of other hydrogen bonds leads to mutual distortions. On this topic, Jeffrey states in a recent authoritative text^{1b} that “In the solid state, the packing of molecules is determined by their shape and a variety of intermolecular forces, of which the hydrogen bond is only one, not necessarily the dominant one. For this reason, more structural variety [of hydrogen bonds] is observed than in gas-phase hydrogen-bonded dimers and adducts.” Indeed, recent work has shown that intermolecular interactions can even lead to substantial and quite significant distortions of covalent bond geometries in the solid state.¹¹

In our previous reports on factors affecting the geometry and strength of N—H···Co hydrogen bonds in $R_3NH^+Co(CO)_3L^-$ ($L = CO, PPh_3$)^{3a,6b-d} salts, we have examined the effect of major changes in either the steric demands of the ammonium cation or the basicity of the anion. Such changes have resulted in corresponding changes in N···Co [and H···Co]¹⁵ separations on the order of 0.15–0.3 Å, as detailed in the Introduction, with decreases in the hydrogen bond length being associated either with decreased cation–anion steric interaction or increased anion basicity. In the present study, we examine the effect of making much smaller molecular changes. Thus, the cations and anions of compounds **1–3** exhibit the same steric characteristics in the proximity of the N—H donor and Co acceptor groups as the previously reported salts, i.e., either **4** or **5**. Corresponding electronic changes in the cation or anion are also very minor (i.e., **1** vs **4**; **2** or **3** vs **5**). However, examination of the N—H···Co hydrogen bond geometries of **1–3** shows that the effect of these minor changes at the molecular level has been overwhelmed in the solid state by the effect of changes at the supramolecular level. Indeed **1–3** all exhibit N—H···Co hydrogen bonds in the solid state that are ca. 0.1–0.15 Å longer than might have been predicted upon consideration only of previous structure determinations coupled with solution spectroscopic data.

Recent work has shown the importance of weak hydrogen bonds such as C—H···O in determining molecular conformations and supramolecular architectures of organic species.¹⁶ Moreover, as the result of exhaustive CSD¹⁷ searches, Braga, Grepioni, Desiraju, and co-workers have demonstrated^{3g,4b} that rather weak but very abundant hydrogen bonds such as C—H···O are important in determining the arrangement of molecules and ions in the crystal structures of transition metal carbonyl complexes. Extensive networks of C—H···O hydrogen bonds are present in the crystal structures of **1–3** (also **4** and **5**). As indicated above, changes in this ensemble of hydrogen bonds is most probably a major contributor to the “unexpected” changes in the N—H···Co geometry in **1–3**.

Since the vast majority of the crystallographic studies are conducted to elucidate the molecular structure, we often tend to ignore or overlook intermolecular interactions occurring in the crystal structure or perhaps more dangerous still focus on the geometry of individual interactions. The conclusions presented here do not pertain only to these systems but have wider implications to the study of all weak interactions in the solid state. In inorganic chemistry, for example, there is much current interest in σ -bond complexes¹⁸ and in a variety of hydrogen bonds that involve transition metals, as noted in the Introduction. Geometries derived from crystallographic char-

acterizations of such weak interactions must inevitably be considered in the context of the overall supramolecular arrangement. As is thus evident from the present study, much more work is needed in order to understand the interrelation of intermolecular interactions. This includes determining the strengths of different types of interactions and examining preferred supramolecular arrangements. Indeed, while the understanding of chemistry and molecular synthesis based upon covalent bonds is a relatively mature discipline, the corresponding understanding and application of intermolecular bonding to supramolecular synthesis^{2a,19} is by contrast still in its infancy.

Finally, in a *Nature* editorial 10 years ago, John Maddox opined²⁰ that “One of the continuing scandals in the physical sciences is that it remains in general impossible to predict the structure of even the simplest crystalline solids from a knowledge of their chemical composition.” This statement is quite pertinent to the present study, though it should not be taken to suggest that no progress has been made in the area of crystal structure prediction. Indeed, in the intervening decade, models have been developed that allow ab initio computation of some crystal structures,²¹ though such models are still far from having universal applicability.^{21f} The diversity of intermolecular interactions, their relatively low energies, and their independence will make such structure prediction a difficult proposition for most compounds for some time to come. The present work clearly reinforces this assertion.

Conclusions

Three new examples of N—H···Co hydrogen-bonded salts involving the tetracarbonylcobaltate(–I) or tricarbonylphosphinecobaltate(–I) anion are reported. Despite the minor differences, at the molecular level, between these salts and previously reported examples, each exhibits a markedly longer (0.1–0.15 Å) hydrogen bond in the solid state than would be predicted based upon previous structure determinations together with spectroscopic evidence in solution. Thus, minor changes at the molecular level are subsumed by major changes at the supramolecular level where the overall energetic balance of intermolecular interactions is important in determining the geometry of any given interaction. This contrasts with our previous reports, in which changes at the molecular level were clearly large enough to dominate the changes in the N—H···Co hydrogen bond even in the solid state. Although, in those cases, the contribution of supramolecular changes to the change in the N—H···Co hydrogen bond geometry was not readily quantified.

- (16) (a) Nishio, M.; Hirota, M. *Tetrahedron* **1989**, *45*, 7201. (b) Nishio, M.; Umezawa, Y.; Hirota, M.; Takeuchi, Y. *Tetrahedron* **1995**, *51*, 8665. (c) Steiner, T. *Crystallogr. Rev.* **1996**, *6*, 1. (d) Desiraju, G. R. *Acc. Chem. Res.* **1996**, *29*, 441.
- (17) Allen, F. H.; Kennard, O. *Chem. Design Automation News* **1993**, *8*, 1, 31–37.

- (18) (a) For a recent review, see: Crabtree, R. H. *Angew. Chem., Int. Ed. Eng.* **1993**, *32*, 789. (b) For a remarkable recent example of a metal–alkane complex, see: Evans, D. R.; Drovetskaya, T.; Bau, R.; Reed, C. A.; Boyd, P. D. W. *J. Am. Chem. Soc.* **1997**, *119*, 3633. The fact that the crystallographically determined Fe···C distances in this complex must be dependent upon the overall energetic balance a variety of intermolecular interactions, in addition to the specific C—H—Fe interaction, is implicitly recognized by the authors of this study, who point out that the complex is stabilized by the cavity in which the alkane resides. Distances calculated for model complexes differ from crystallographic values by ca. 0.1–0.2 Å.
- (19) Desiraju, G. R., Ed. *Perspectives in Supramolecular Chemistry: The Crystal as a Supramolecular Entity*; Wiley: Chichester, 1996; Vol. 2.
- (20) Maddox, J. *Nature* **1988**, *335*, 201.
- (21) For example see: (a) Gavezotti, A. *J. Am. Chem. Soc.* **1991**, *113*, 4622. (b) Karfunkel, H. R.; Gdanitz, R. J. *J. Comput. Chem.* **1992**, *13*, 1171. (c) Perlstein, J. *J. Am. Chem. Soc.* **1992**, *114*, 1955. (d) Perlstein, J. *J. Am. Chem. Soc.* **1994**, *116*, 11420. (e) Price, S. L.; Wibley, K. S. *J. Phys. Chem. A* **1997**, *101*, 2198. (f) Gavezotti, A. *Acc. Chem. Res.* **1994**, *27*, 309.

In the present structures, one cannot expect to identify a specific change in supramolecular arrangement as the cause of the lengthened N–H···Co hydrogen bonds. However, one can point to probable causes. In **1**, a hydrogen bond acceptor group (N) has been replaced by donor group (C–H) relative to the previously studied **4**, and both acceptor in **4** and donor in **1** are active in hydrogen bonding. In **2** and **3**, replacement of phenyl substituents by *p*-tolyl groups and the incorporation in the solid state of molecules of acetonitrile solvate represent the most obvious differences between these structures and that of the previously studied **5**. Thus, while the “lengthening” of the N–H···Co hydrogen bonds in **1–3** may seem at first unexpected, it can be rationalized in terms of the collective effect of often overlooked weak intermolecular interactions.

Note Added in Proof

It is noted that the acidities of (Quin)H⁺ and (DABCO)H⁺ are not identical. The former is less acidic by ca. 0.5 p*K*_a units. This may contribute in part to the fact that the N–H···Co hydrogen bond is longer in **1** than in **4**.

Acknowledgment. Financial support from the Donors of the Petroleum Research Fund, administered by the American Chemical Society, the Missouri Research Board, and an UMSL Research Award, is acknowledged. J.C.M.R. acknowledges further support in the form of fellowships from the UMSL chemistry alumni, the UMSL graduate school, and Mallinckrodt Chemical Co. The Bruker ARX-500 NMR spectrometer was purchased with support from the U.S. Department of Energy, Grant No. DE-FG02-92CH10499. Purchase of the Bruker (Siemens) SMART diffractometer was funded in part by NSF Grant No. CHE-9309690.

Supporting Information Available: Tables of crystallographic data, positional and displacement parameters, interatomic distances, and angles for **1–3** and figure S1 showing the disorder model for **3** (18 pages). Crystallographic data for **1–3**, in CIF format, are available on the Internet only. Ordering and access information is given on any current masthead page.

IC980317O